

SEEING THE LIGHT - CATCHING THE WIND

Technological Advances in Optical Air Data Systems

Rao Tatavarti¹, Arulmozhivarman P.², Kishore M.P.K. ¹, Anil Kumar J.¹, Sanjay Sarma O.V.¹ Aparna T.³

¹Gayatri Vidya Parishad Scientific and Industrial Research Centre,
GVP College of Engineering Campus, Madhurawada, Visakhapatnam 530048, India
²School of Electronics Engineering, VIT University, Vellore 632014, India
³GVP College of Engineering for Women, Madhurawada, Visakhapatnam 530048, India

ABSTRACT

The impetus for the current research and development towards the realization of a remote monitoring, non-intrusive sensing system for real time monitoring of the environment, stems from the many challenges and constraints faced by the civilian and defence users of conventional technologies. The focus of the current work is on adopting innovative approaches in the design and development of a photonics based system for real time determination of the free air stream velocity, with higher degree of sensitivity and accuracy. The photonics system can be suitably modified for applications onboard automobiles, aircrafts and underwater platforms.

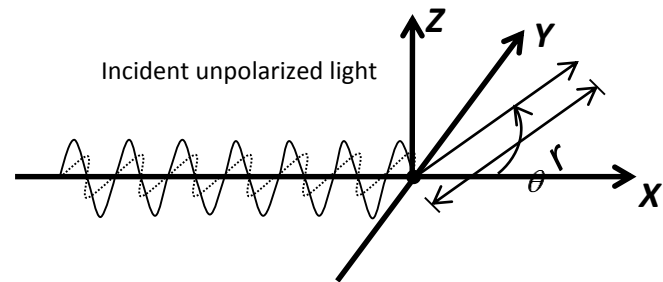
Index Terms — Photonics, Optoelectronics, Scattering of Light, Sensor, Fluid, Monitoring, Moving Platforms.

1. INTRODUCTION

The need for a highly sensitive non-intrusive sensor for monitoring stratified fluids in the real world from moving platforms like aircrafts in the atmosphere or submerged bodies in the ocean was the impetus for this work. Recent research focuses on the use of optical scattering as a promising mechanism for fluid monitoring [1-4]. Although these sensors are highly promising, with multinational defense industries are working towards perfecting the technologies involved, in addition to developing highly sensitive aircraft based systems - the systems essentially require accurate optics, and their perfect alignments with precision engineering for yielding good results in real time. Most of the efforts around the world, also necessitate huge costs and complex optical configurations where in substantial space needs to be allocated for the systems onboard aircrafts [5, 6]. As is well known space for scientific systems on board aircrafts, especially defense aircrafts, is always a premium. Against this background we attempted to look at the utility of the concepts of forward scattering as well as back scattering of light for monitoring fluids in stratified fluids like the atmosphere, and ocean.

2. SCATTERING OF LIGHT BY AIR MOLECULES AND AEROSOLS: RAYLEIGH SCATTERING

Light is an electromagnetic radiation, comprising of electric and magnetic fields. The electric field for a plane polarized light traveling along z-axis is given by $E_z = E_0 \cos(\omega t)$, where E_0 is the amplitude of the electric field at origin, ω is the oscillating frequency.



Considering the case of light falling on some scatterers (particles) we can show that a dipole moment is generated by the light falling on a scatterer (particle) *per se*. If the particle is polarizable, then the incident electric field will induce a dipole moment in the particle which would be in the same direction as the incident field polarization and is linearly proportional to the incident electric field. Say, the scalar constant of proportionality called polarizability is α_p , then the dipole moment can be expressed as $p = \alpha_p E_0 \cos(\omega t)$. It can also be shown that the scattered light field will be proportional to $\frac{1}{c^2} \left\{ \frac{d^2 p}{dt^2} \right\}$, where c is the speed of the light; $\left\{ \frac{d^2 p}{dt^2} \right\}$ is the acceleration of the charge on the dipole moment. To include the spatial effects, the scattering light is proportional to $1/r$ and $\sin(\theta_z)$ where r is the distance measured from origin to the point of observation of scattering of light, θ_z is the angle the observing direction makes with z-axis. Combining all these effects the scattered light in θ_z direction is given by

$$E_s = \frac{1}{r} \frac{1}{c^2} \sin(\theta_z) \left\{ \frac{d^2 p}{dt^2} \right\} = -\frac{1}{r} \frac{1}{c^2} \alpha_p E_0 \omega^2 \sin(\theta_z) \cos(\omega t)$$

$\Rightarrow E_s = -\alpha_p E_0 \frac{4\pi^2}{r\lambda^2} \sin(\theta_z) \cos\left(\frac{2\pi c}{\lambda} t\right)$, where $\lambda = 2\pi c / \omega$ is the wavelength.

The intensity of the electric field is given by $I_s = |E_s|^2$;

$\Rightarrow I_s = \alpha_p^2 I_{oz} \frac{16\pi^4}{r^2 \lambda^4} \sin^2(\theta_z)$; where $I_{oz} = E_o^2$ is the intensity of the z polarized incident light. For an unpolarized light traveling in x direction, the incident intensity becomes $I_o = \frac{1}{2} I_{oz} + \frac{1}{2} I_{oy}$, where I_{oz} and

I_{oy} are the incident light polarized in both z direction and y direction respectively. The scattered light intensity is given by

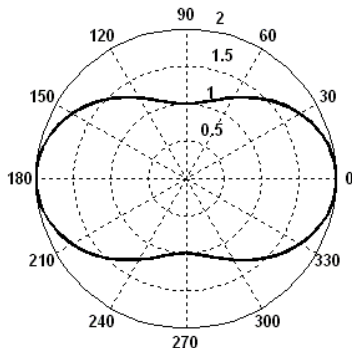
$I_s = \frac{1}{2} I_{sz} + \frac{1}{2} I_{sy} = I_o \frac{8\pi^4 \alpha_p^4}{r^2 \lambda^4} (\sin^2 \theta_z + \sin^2 \theta_y)$, where θ_y is the angle the observing direction makes with y-axis. Using geometry θ_z and θ_y terms can be related

$\theta(=\theta_y)$ as $\cos^2 \theta + \cos^2 \theta_y + \cos^2 \theta_z = 1 \rightarrow \sin^2 \theta_y + \sin^2 \theta_z = 1 + \cos^2 \theta$.

Hence, $I_s = I_o \frac{8\pi^4 \alpha_p^4}{r^2 \lambda^4} (1 + \cos^2 \theta)$. Assuming that the volume of scattering comprises of many particles (scatterers), we have for n moles of particle or nL particles (L is the Avogadro number) in a volume V, the scattering intensity at θ is

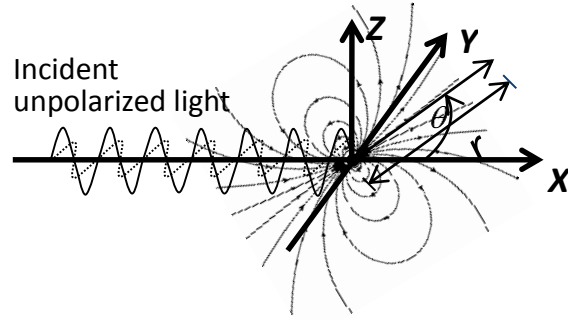
$$I_\theta^o = \frac{I_o nL}{V} \frac{8\pi^4 \alpha_p^4}{r^2 \lambda^4} (1 + \cos^2 \theta)$$

The subscript on I denotes scattering due to small particles. Therefore, the light scattering intensity depends on the scattering angle. The shape of the diagram is determined by the $(1 + \cos^2 \theta)$ term as shown below.



Scattered Intensity Distribution

The maximum scattering intensity is at $\theta = 0^\circ$ and the minimum scattering intensity is at $\theta = 90^\circ$. The effect of Rayleigh scattering of light due to air molecules and aerosols (scatterers) is shown in the following schematic.



3. NON INVASIVE PHOTONICS SYSTEM FOR MONITORING FLUIDS

The photonics system for real time monitoring of stratified fluids (for example atmosphere and oceans) comprises of a continuous wave, coherent, collimated beam of light (or a laser) falling on the surface of a photo detector in such a way that the received light falls partially on the active sensing area of the photo detector and partially on the encapsulation of the photo detector, after passing through the stratified fluid medium (Figure 1). The light intensity falling on the photo detector undergoes changes due to changes in the optical refractive gradient generated as a result of fluid motions in the stratified fluid. The photo detector records the precise time varying light intensity pattern, corresponding to the time varying motions experienced in the stratified fluid due to motions. The output signals from the photo detector are recorded and compared with those obtained from a standard sensor. The efficacy of this method and system for real time monitoring of stratified fluids was demonstrated.

The relationship between the optional refractive index and the temperature (density) of a fluid is given by the Gladstone-Dale Equation, $n = 1 + \kappa\rho$ (the optical refractive index is linearly related to fluid density) where, n is the optical refractive index, ρ the density of the fluid and κ is a constant coefficient which is a function of the laser wavelength and the fluid characteristics. Therefore, the refractive index gradient is linearly related to temperature (density) gradient or the change in refractive index gradient will yield the change in density gradient of a fluid (see Figure 2). Based on this concept, it can be inferred as follows, as suggested by Tatavarti *et al.* [7]:

$$\epsilon_x = \int \frac{1}{n} \frac{\partial n}{\partial x} dz$$

$$\delta_x = \frac{L}{n} \frac{\partial n}{\partial x} \approx \frac{L}{\rho} \frac{\partial \rho}{\partial x}$$

$$\epsilon_y = \int \frac{1}{n} \frac{\partial n}{\partial y} dz$$

$$\delta_y = \frac{L}{n} \frac{\partial n}{\partial y} \approx \frac{L}{\rho} \frac{\partial \rho}{\partial y}$$

where, L is the optical path length of the beam in fluid and x and y are horizontal and vertical co-ordinates. The dimensions δ_y of are $m/(Kg/m^3) \times (Kg/m^3)/m$. Therefore, δ_y will be dimensionless.

For the optoelectronic systems the minimum resolvable δ (an artefact of the sensitivity of the position sensing detector used), say, $0.1\mu m = 1 \times 10^{-7}m$; an optical path length L designed as, say, $0.1m$; $\partial_y = 1m$; and an average density value of ρ (air) $\approx 1Kg/m^3$. For calculating the minimum resolvable $\Delta\rho$ (ΔT) we have

$$\frac{\delta_y \rho}{L} = \frac{\partial \rho}{\partial y}$$

i.e., the minimum resolvable $\Delta\rho$ is, $O(10^{-6}) Kg/m^3$ (or the minimum resolvable temperature is $0.001^\circ C$).

Hence, the sensitivity and accuracy of the optoelectronic sensor system for monitoring fluid parameters using the concept of forward light scattering, are extremely good (orders of magnitude higher) compared to conventional existing technologies, and the same can be realized, with position sensing detectors of sub-micron accuracy and sensitivity.

It is well documented [8] that changes in the environment in which a light beam is traversing can be realistically monitored with increased sensitivity (compared to conventional sensing mechanisms) if one could study the optical diffraction and interference fringes which are manifest. However, to observe these fringes one needs to make elaborate design involving complex optical configurations and precise optical alignments. Tatavarti and Santhanakrishnan [9] have patented a simpler method to simultaneously generate and detect the diffraction fringes caused due to changes in the environment, and the same is used in this study. Therefore, in order to further increase the sensitivity and the dynamic range of sensing we ensure that the laser beam is focused in such a way that forward or backscattered light falls partially on the active sensing area of the detector, and partially on the outer perimeter of the active sensing area of the photo detector, thus ensuring a spatial intensity pattern on the photo detector [9].

4. EXPERIMENTAL INVESTIGATIONS

Light from a laser diode modulates due to the changes in fluid velocity and temperature, following the principle of Laser beam deflection and forward scattering of light. The modulated light signals are allowed to fall on the edge of the photo detector, thus ensuring generation of diffraction fringes due to interference between the direct light on the active sensing area and the diffracted light from the edge of the photo detector. The photo detector

used is a position sensing photo diode which converts the light energy into electrical energy and gives the light intensity and position on the detector. The signals from the photodiode are processed using a simple algorithm on board a computer which yields information regarding the fluid velocity and temperature. Experiments were conducted with a small fan capable of blowing air at three speeds (7cm/s, 10.5cm/s, 12.6cm/s); and an warm air blower (hair dryer) capable of blowing warm air at constant speed of 0.5m/s with different temperature settings of $40^\circ C$, $60^\circ C$ and $80^\circ C$. The speeds of the fan and the temperatures of the air blower were measured using standard procedures and instruments. The experiments were conducted with different configurations to monitor the effect of blowing air at different speeds at room temperature, and blowing air at constant velocity with different temperatures. The geometry and speeds of the air emanating from both the Fan and the hair dryer were different. During the experiments the laser source and the photo detector were separated by 0.5m, while the Fan/Warm Air Blower were located about 2cm, perpendicularly facing the laser beam.

The laboratory setup during the experiments for demonstrating the mechanism of the sensor is pictured in Figure 3. A diode laser of 5mW of 635 nm was used as the source of light. A 2-D position sensing silicon photo diode with a positional resolution of $0.1\mu m$ was used as the photo detector. The light beam from the laser diode was made to fall on the edge of the photo detector, with the beam falling partially on the active sensing area and partially on the outer perimeter of the photo detector. This ensured a higher signal to noise ratio and a high dynamic range during detection as was earlier demonstrated [9] The geometry of the 2D position sensing photo detector vis-à-vis the position of the fan and the warm air blower (hair dryer) is shown in Figure 4. The air flow was towards the negative x -direction of the photo detector. The y -direction is considered positive upwards.

Figure 5 shows the field setup of an experiment conducted atop a hill in Visakhapatnam to demonstrate the efficacy of the back scattering technique developed based on the theoretical investigations. Observations were recorded by connecting a data acquisition system to the 2-D position sensing photo detector and selecting a data sampling rate of 16Hz, and quantizing the signals with 16 bit resolution. Data were observed during different phases with various air speeds at ambient temperature and with different temperatures at constant air speed. The output from the photo detector is obtained in terms of the beam deflections in microns from the reference origin in the x and y directions during different experimental phases (δ_x , δ_y).

5. RESULTS AND DISCUSSION

Figure 6 shows the time averaged (1-sec) data clusters of x and y deflections (δ_x, δ_y) of the laser beam due to various air speeds generated by the fan at room temperature. Figure 6 show the time averaged (1-sec) data clusters of x and y deflections (δ_x, δ_y) of the laser beam due to various temperatures generated by the air blower at constant air speed. The linear regression plots and the corresponding relations between (δ_x, δ_y) are also shown in the figures. Centroids of each of the data cluster corresponding to various phases of the experimental observations (changing air speeds and temperatures) were determined using the K-Means method and depicted as squares (grey in color) in the Figures 6 and 7. Based on the observed data clusters, regression equations and the computed centroids a simple signal processing algorithm, whose flow chart is shown in Figure 7, determines the fluid velocity and temperature. The derived equations for determining the fluid velocity and temperature are as follows:

$$u = -0.416731d^2 + 4.592204d - 0.021443 \text{ (cm/s)}$$

where, $d = (\delta_{x_i} - \delta_{y_i}), (\delta_{x_i}, \delta_{y_i})$ are the instantaneous values, ($\delta_{x_0}, \delta_{y_0}$) are the reference values.

Figure 8 demonstrates the efficacy of the back scattering technique for determining the free air stream velocity. The independent wind measurement with a conventional anemometer is superimposed on the graph. It should be noted that the conventional anemometer used for monitoring the wind velocity is far less sensitive and additionally has constraints in the sampling of data. The preliminary results indicated that the sensitivity and accuracy of the photonics system under development are better, compared to conventional standard intrusive sensors.

Efforts are underway to further improve the algorithm for determination of the free air stream velocity as well as demonstrate the robustness and repetitive nature of the photonics system under controlled conditions as well as additional field experiments.

6. CONCLUSIONS

A non-invasive and sensitive optoelectronic technique for the design and development of a sensor for mobile platforms for real time monitoring of surrounding fluid velocity, temperature (density) which can be adapted for use on board moving aircrafts or underwater platforms like ROVs, torpedoes, ships and submarines is demonstrated.

7. REFERENCES

[1] Srivastava A. (2010). Calibration of flush air data sensing systems using surrogate modeling techniques, *PhD Thesis*, Rice University, Houston, Texas, USA.
 [2] Hays, P. B. (2006). Molecular Optical Air Data Systems (MOADS), Michigan Aero Space Corporation, USA, *United States Patent US 7106447 B2*.
 [3] Perry J., Mohammed A., Johnson, B., and Lind, R. (2008). Estimating angle of attack and sideslip under high dynamics on small UAVs , *Proc. ION GNSS 21st International Technical Meeting of Satellite Division*, Savannah, GA, USA, p. 1165 - 1173.
 [4] Modares D., Gharib M., and Taugwalder F. (2003). Miniature optical sensor, California Institute of Technology, USA, *United States Patent, US 6654102 B1*.
 [5] Gharib M., Wilson D.W., Forouhar, S., Muller R.E., Fourgette, D., Modarress D., and Taugwalder F., (2004). Diffractive optical fluid shear stress sensor, California Institute of Technology, USA, *United States Patent, US 6717172 B2*.
 [6] Valla M., Besson C., and Augere B. (2012). Measurement of speed or vibration characteristics using a Lidar device with heterodyne detection, Onera, France, *United States Patent, US 8179521 B2*.
 [7] Rao Tatavarti, P.N. Ananth, K. Rajasree, V. Vidyalal, P. Radhakrishnan, V.P.N. Nampoori, and C.P.G. Vallaban (1995). Internal waves: A novel measurement technique, *Current Science*, Vol.69, No. 8, p.678-684.
 [8] Gharib M., Fourgette, D., Modarress D., Taugwalder F., and Forouhar, S. (2005). Integrated particles sensor formed using fringes formed by diffractive elements, California Institute of Technology, USA, *United States Patent, US 6956230 B1*.
 [9] T Santhanakrishnan and Rao Tatavarti (2010). Method and apparatus for the simultaneous generation and detection of the optical diffraction pattern of detector, *United States Patent, US 2010/0321698 A1*.

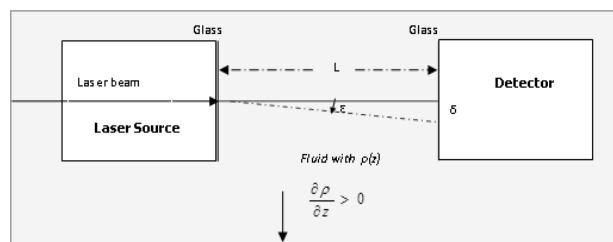


Figure 1: Laser beam deflection in a density stratified fluid

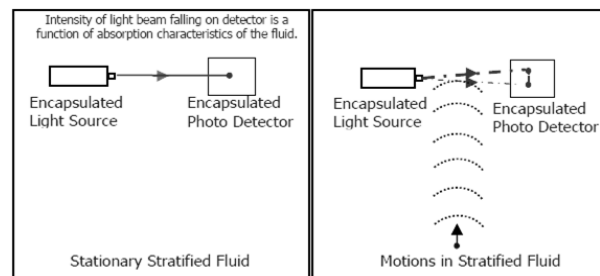


Figure 2: Schematic description of the working principle of photonics system for monitoring stratified fluid motions.

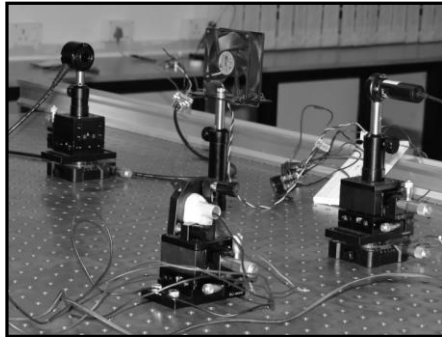


Figure 3: Laboratory setup for demonstration of the proposed system.

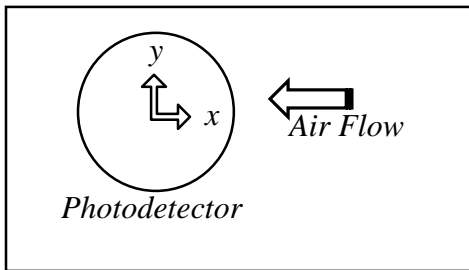


Figure 4: Geometry of the photo detector vis-à-vis the air flow direction from fan / blower

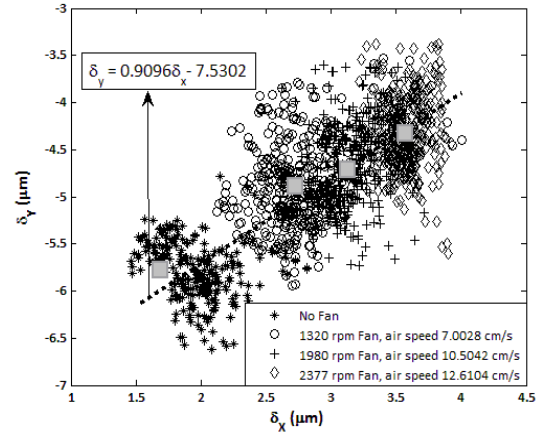


Figure 6: Observed data cluster of (δ_x, δ_y) for different air speeds.

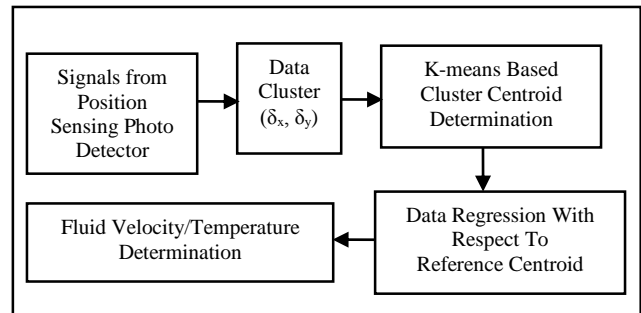


Figure 7: Block diagram of the signal processing algorithm for determination of fluid velocity and temperature (density).

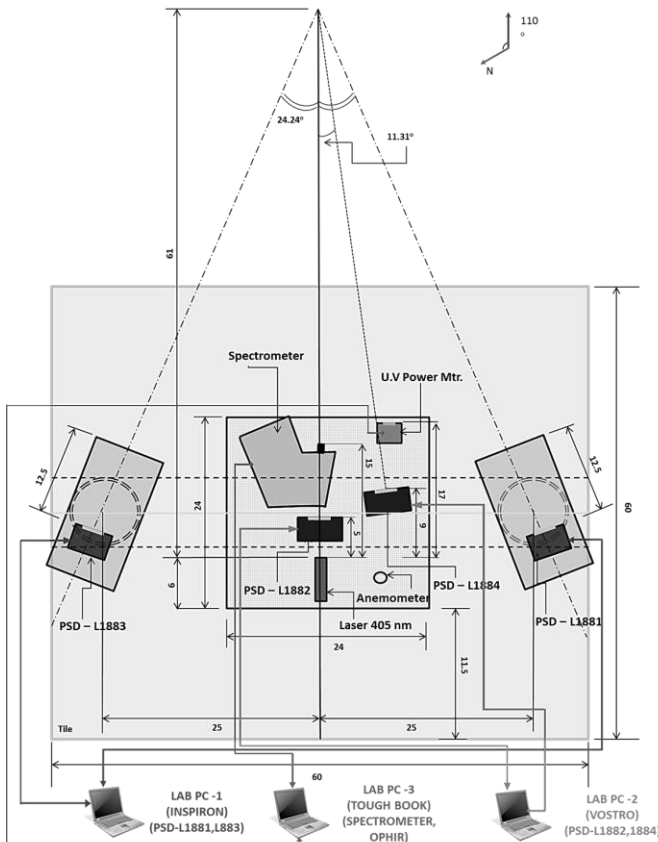


Figure 5: Schematic of the set up during field experiment for monitoring free air stream velocity.

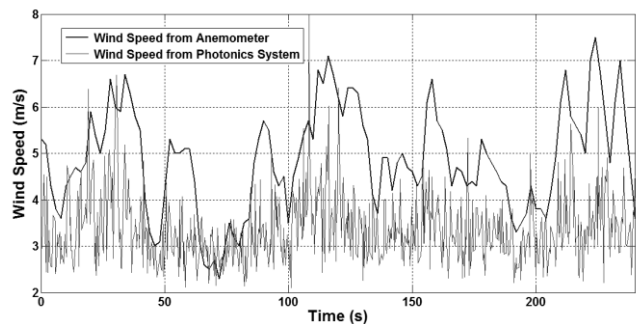


Figure 8: Wind Speed as measured by conventional anemometer (with constraints in sampling and sensitivity) and the photonics system under development.